



Amortizing Maximum Inner Product Search with Learned Support Functions

Theo X. Olausson^{2†}, João Monteiro¹, Michal Klein¹, Marco Cuturi¹

¹Apple, ²MIT, [†]Work done during Apple internship.

Maximum inner product search (MIPS) is a crucial subroutine in machine learning, requiring the identification of key vectors that align best with a given query. We propose *amortized MIPS*: a learning-based approach that trains neural networks to directly predict MIPS solutions, amortizing the computational cost of matching queries (drawn from a *fixed* distribution) to a *fixed* set of keys. Our key insight is that the MIPS value function, the maximal inner product between a query and keys, is also known as the *support* function of the set of keys. Support functions are convex, 1-homogeneous and their gradient w.r.t. the query is exactly the optimal key in the database. We approximate the support function using two complementary approaches: (1) we train an input-convex neural network (SupportNet) to model the support function directly; the optimal key can be recovered via (autodiff) gradient computation, and (2) we regress directly the optimal key from the query using a vector valued network (KeyNet), bypassing gradient computation entirely at inference time. To learn a SupportNet, we combine score regression with gradient matching losses, and propose homogenization wrappers that enforce the positive 1-homogeneity of a neural network, theoretically linking function values to gradients. To train a KeyNet, we introduce a score consistency loss derived from the Euler theorem for homogeneous functions. Our experiments show that learned SupportNet or KeyNet achieve high match rates and open up new directions to compress databases with a specific query distribution in mind.

Correspondence: Theo X. Olausson: theo@csail.mit.edu; João Monteiro: joaomonteirof@apple.com; Michal Klein: michal_klein2@apple.com; Marco Cuturi: m_cuturi@apple.com.

1 Introduction

Maximum inner product search (MIPS) is a fundamental subroutine within numerous machine learning blocks. Given a query vector $\mathbf{x} \in \mathbb{R}^d$ and a database of vectors $\mathcal{Y} = \{\mathbf{y}_1, \dots, \mathbf{y}_n\} \subset \mathbb{R}^d$, the goal of MIPS is to identify the vector in \mathcal{Y} that maximizes the inner product with \mathbf{x} :

$$\mathbf{y}^*(\mathbf{x}) = \arg \max_{\mathbf{y} \in \mathcal{Y}} \langle \mathbf{x}, \mathbf{y} \rangle. \quad (1.1)$$

While this problem is typically solved exhaustively by leveraging GPU parallelism in $O(nd)$ time, this becomes computationally prohibitive when dealing with large-scale datasets containing millions of high-dimensional vectors. Yet, MIPS plays a crucial role in various domains, including recommendation systems [Bachrach et al. \(2014\)](#); [Koenigstein et al. \(2012\)](#), information retrieval [Shrivastava and Li \(2014\)](#), natural language processing [Guo et al. \(2016\)](#), and neural network inference [Chen et al. \(2015\)](#).

Approximate MIPS. The computational challenge posed by large-scale MIPS has motivated extensive research into *approximate* MIPS methods, which trade a small amount of accuracy for significant computational savings ([Jégou et al., 2011](#)). These approaches typically rely on indexing structures (hashing, trees, graphs) or quantization schemes that must be queried at inference time. While effective, they do not leverage information about the *query distribution*—queries are treated as arbitrary vectors, even when applications exhibit predictable query patterns.

Amortized MIPS: A Learning Perspective. We propose a fundamentally different approach: Rather than building query-agnostic indexing structures, we train networks to directly predict MIPS solutions, amor-

tizing the computational cost of search across queries drawn from a known distribution \mathcal{X} . The key insight underlying our approach is that the MIPS *value function*—the max inner product—is the *support function* of the database \mathcal{Y} :

$$\sigma_{\mathcal{Y}}(\mathbf{x}) = \max_{\mathbf{y} \in \mathcal{Y}} \langle \mathbf{x}, \mathbf{y} \rangle, \quad (1.2)$$

This function is convex (as the pointwise maximum of linear functions) and positively 1-homogeneous. Moreover, by the envelope theorem, its gradient at each query equals the optimal database vector: $\nabla \sigma_{\mathcal{Y}}(\mathbf{x}) = \mathbf{y}^*(\mathbf{x})$. These structural properties of the support function motivate two learning paradigms: either train a network to predict the real-valued function directly (SUPPORTNET) or to predict the top key (KEYNET). We propose to ground the training of SUPPORTNET on loosely-constrained input convex neural networks (ICNNs) (Amos et al., 2017), to learn the convex support function as $f_{\theta}(\mathbf{x}) \approx \sigma_{\mathcal{Y}}(\mathbf{x})$. We can then recover an approximation of the optimal key via a backward gradient computation (w.r.t. \mathbf{x}) of $\nabla_{\mathbf{x}} f_{\theta}(\mathbf{x})$. Training KEYNET can be done instead by regressing directly the optimal key $F_{\theta}(\mathbf{x}) \approx \mathbf{y}^*(\mathbf{x})$, bypassing backward computation entirely at inference. It is important to note that in both cases, ours is an example of amortized optimization: we will consider throughout the work that we have access, for any query \mathbf{x} sampled from a relevant distribution of queries $p_{\mathcal{X}}$, to its ground truth score $\sigma_{\mathcal{Y}}(\mathbf{x})$ and ground-truth key $\mathbf{y}^*(\mathbf{x})$ by running AMIPS on that dataset. Our contributions are:

- We introduce SUPPORTNET and KEYNET, two models and their regression-based training approach to amortize AMIPS. We design loss functions for both: score regression and gradient matching for the first, multivariate regression and *score consistency*, based on Euler’s theorem for homogeneous functions, for the latter.
- We propose *multi-task* extensions of these two approaches when learning multiple MIPS tasks *jointly*, using parameter sharing. This is useful to address problems where the keys can be partitioned into clusters, but are queried using queries sampled from the same distribution. We show how these support functions learned jointly can be used to identify to which cluster a query should be matched, without running any comparisons with the keys in those clusters.
- We demonstrate on retrieval benchmarks that amortized MIPS achieves high match rates, and that modifying queries using learned models improves recall of standard approximate search indices. We consider two scenarios where support function and the top-key predictors are respectively highlighted: We cluster the keys into subgroups and train (jointly) as many support functions, and use this as a routing mechanism; we convert a query into its predicted key and test whether fast AMIPS search with the predicted key returns better results than when run with the original query. In both cases we observe significant speedups (factoring accuracy vs. FLOPS) across a wide range of hyperparameters for our architectures.

2 Background

Maximum Inner Product Search. The exact search required to compute either equation 1.2 or equation 1.1 requires $O(nd)$ time, which can be prohibitive for large-scale applications. Approximate MIPS methods fall into several categories. *Transformation-based* approaches convert MIPS to nearest neighbor search via augmented embeddings Shrivastava and Li (2014); Bachrach et al. (2014); Neyshabur and Srebro (2015). The key insight is that inner products can be encoded as Euclidean distances in a higher-dimensional space, enabling the use of efficient nearest neighbor algorithms. *Quantization methods* compress database vectors for fast approximate inner products Jégou et al. (2011); Guo et al. (2016, 2020). Product quantization and its variants decompose vectors into sub-vectors, each quantized independently, achieving significant compression while maintaining reasonable accuracy. *Graph-based* methods construct proximity graphs for greedy traversal Morozov and Babenko (2018); Malkov and Yashunin (2020). These approaches build navigable small-world graphs where edges connect vectors with high mutual inner products, enabling efficient beam search at query time. *Learning-to-hash* approaches train neural networks to produce binary codes preserving inner product structure Dai et al. (2020); Shen et al. (2015). Recent work has also explored learned indices that adapt to data distributions Kraska et al. (2018). All these methods build query-agnostic index structures; our approach differs by learning query-dependent mappings that exploit the distribution of queries.

Input Convex Neural Networks (ICNN) ICNNs are neural architectures guaranteed to be convex in

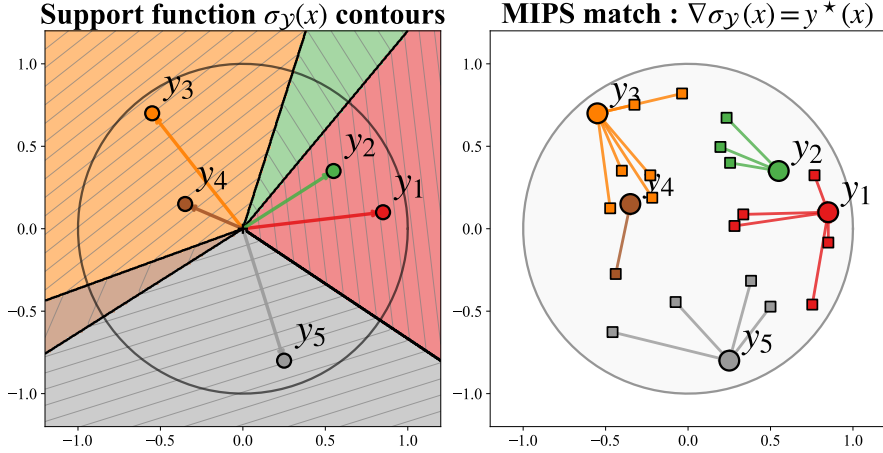


Figure 1 In this figure, the set \mathcal{Y} of keys (shown as dots) consists of 5 points. The support function, represented as a contourplot on the left, is a convex, piecewise-linear function of the query \mathbf{x} . The gradient $\nabla\sigma_{\mathcal{Y}}(\mathbf{x})$ at any query equals the database point \mathbf{y}^* that maximizes $\langle \mathbf{x}, \mathbf{y} \rangle$. The gradient $\nabla_{\mathbf{x}}\sigma_{\mathcal{Y}}(\mathbf{x})$ is exactly the key to which a query is matched (here represented as small squares). While SUPPORTNET is trained to model the contour plot on the left (modeling a piecewise affine function), KEYNET is trained to map inputs to optimal keys directly, as shown on the right plot (a piecewise constant vector-valued function).

their inputs Amos et al. (2017). An ICNN with L layers computes:

$$\begin{aligned} \mathbf{z}_1 &= \sigma \left(\mathbf{W}_0^{(x)} \mathbf{x} + \mathbf{b}_0 \right) \in \mathbb{R}^h, \\ \mathbf{z}_{i+1} &= \sigma \left(\mathbf{W}_i^{(z)} \mathbf{z}_i + \mathbf{W}_i^{(x)} \mathbf{x} + \mathbf{b}_i \right) \in \mathbb{R}^h, \quad 1 \leq i \leq L-1, \\ f(\mathbf{x}) &= \mathbf{z}_L \in \mathbb{R} \end{aligned}$$

where σ is a convex, monotonically non-decreasing activation (e.g., ReLU, softplus), and crucially, $\mathbf{W}_i^{(z)} \geq 0$ element-wise. The non-negativity ensures that each layer preserves convexity. The “passthrough” connections $\mathbf{W}_i^{(x)} \mathbf{x}$ (with unconstrained weights) provide expressiveness, allowing ICNNs to universally approximate continuous convex functions Chen et al. (2019). To train ICNNs, the nonnegativity constraint on the $\mathbf{W}_i^{(z)}$ matrices can be either enforced using clipping (or a softer rectifier, e.g. softplus) so that it only contains non-negative values after each update, or loosely satisfied by adding a regularizer that penalizes negative values, such as $\sum_i \|\text{ReLU}(-\mathbf{W}_i^{(z)})\|^2$. We use the latter approach and combine it with the principled initialization offered by (Hoedt and Klambauer, 2023), which initializes these weight matrices with non-negative values.

Connection to Optimal Transport. Brenier’s theorem establishes that the optimal transport (OT) map between two probability distributions (under squared Euclidean cost) is always achieved by the gradient of a convex function. This has motivated substantial work on learning convex potentials to estimate optimal transport maps from samples Makkuva et al. (2020); Korotin et al. (2021); Amos (2023); Bunne et al. (2022); Korotin et al. (2023). Conversely, that theorem also states that the gradient of a convex function is the optimal map linking any source distribution to the image of that distribution using that gradient. Our amortized MIPS problem has therefore an interesting connection to OT: Indeed, the mapping $\mathbf{x} \mapsto \mathbf{y}^*(\mathbf{x}) = \nabla\sigma_{\mathcal{Y}}(\mathbf{x})$ is, by definition, the gradient of a convex function (the support function), making it a Brenier map. However, very much unlike the typical OT setting where one must *discover* that potential function, in MIPS we have direct access to ground-truth examples of the Brenier potential and its gradient: for any query \mathbf{x} , we can compute its optimal match $\mathbf{y}^*(\mathbf{x})$ via exhaustive search, giving us a gradient, and the dot-product with \mathbf{x} , the potential. As a result, amortized MIPS can be seen as supervised OT learning problem.

3 Methods: Neural Amortized MIPS

We propose *amortized maximum inner product search*: a learning-based approach that trains neural networks to directly predict MIPS solutions. Rather than building indexing structures or hashing schemes that must be queried at inference time, we train a neural network to encode information about the MIPS solution directly in its functional form, amortizing the computational cost of search across queries.

Properties of Support Functions. The MIPS value function equation 1.2, which gives the maximum inner product within a set of keys \mathcal{Y} as a function of the query \mathbf{x} , is the *support function* of \mathcal{Y} . Support functions are fundamental objects in convex analysis Rockafellar (1970); Hiriart-Urruty and Lemaréchal (2004). For any set \mathcal{Y} , $\sigma_{\mathcal{Y}}$ is convex (as the pointwise maximum of linear functions) and positively 1-homogeneous: $\sigma_{\mathcal{Y}}(\alpha\mathbf{x}) = \alpha\sigma_{\mathcal{Y}}(\mathbf{x})$ for $\alpha > 0$. By the envelope theorem, the gradient of the support function at \mathbf{x} equals the maximizing element: $\nabla\sigma_{\mathcal{Y}}(\mathbf{x}) = \mathbf{y}^*(\mathbf{x})$. Figure 1 illustrates this relationship.

Learning Targets. This connection between the support function and its gradient motivates two complementary approaches: SUPPORTNET learns a (real-valued) convex potential that mimics the support function directly on samples that matter: $f_{\theta} : \mathbb{R}^d \rightarrow \mathbb{R}$ is such that $f_{\theta}(\mathbf{x}) \approx \sigma_{\mathcal{Y}}(\mathbf{x})$ for \mathbf{x} that *matter*, i.e. sampled according to $p_{\mathcal{X}}$. The optimal key can be then recovered via $\nabla_{\mathbf{x}}f_{\theta}(\mathbf{x})$ computed using automatic differentiation. KEYNET learns to produce instead, directly, a vector-valued function $F_{\theta} : \mathbb{R}^d \rightarrow \mathbb{R}^d$ that approximates the predicted optimal key $F_{\theta}(\mathbf{x}) \approx \mathbf{y}^*(\mathbf{x})$ for \mathbf{x} sampled according to $p_{\mathcal{X}}$. The support function can be then approximated as $\langle F_{\theta}(\mathbf{x}), \mathbf{x} \rangle$.

Clustered Variants. In many applications, a very large database \mathcal{Y} can be naturally partitioned into c clusters $\mathcal{Y}_1, \dots, \mathcal{Y}_c$ (e.g. using k -means clustering). Rather than learning a single support function for each of these clusters, we propose to cast this joint learning as a multi-task learning problem in which a collection of support functions is learned by sharing parameters. As a result, the goal is to simultaneously learn the support functions for all clusters:

$$\sigma_{\mathcal{Y}_j}(\mathbf{x}) = \max_{\mathbf{y} \in \mathcal{Y}_j} \langle \mathbf{x}, \mathbf{y} \rangle, \quad j = 1, \dots, c. \quad (3.1)$$

This enables a two-stage search: first identify promising clusters via the learned scores, then search exhaustively within those clusters. We describe how both SUPPORTNET and KEYNET extend to this multi-output setting below. The single-output case corresponds to $c = 1$.

3.1 Model Architectures

SupportNet: ICNN-based Architecture. SUPPORTNET uses an Input Convex Neural Network (ICNN) architecture that guarantees the convexity of each of the c output values of $f_{\theta}(\mathbf{x})$ w.r.t. \mathbf{x} Amos et al. (2017):

$$\begin{aligned} \mathbf{z}_1 &= \sigma(\mathbf{W}_0^{(x)}\mathbf{x} + \mathbf{b}_0) \in \mathbb{R}^h \\ \mathbf{z}_{i+1} &= \sigma(\mathbf{W}_i^{(z)}\mathbf{z}_i + \mathbf{W}_i^{(x)}\mathbf{x} + \mathbf{b}_i) \in \mathbb{R}^h, \\ f_{\theta}(\mathbf{x}) &= \mathbf{W}_L\mathbf{z}_L + \mathbf{b}_L \in \mathbb{R}^c, \end{aligned}$$

where $\mathbf{W}_i^{(z)} \geq 0$ (element-wise non-negative), and σ is a convex non-decreasing activation. The ‘‘passthrough’’ connections $\mathbf{W}_i^{(x)}\mathbf{x}$ provide expressiveness while the non-negativity constraint on $\mathbf{W}_i^{(z)}$ ensures convexity is preserved through composition. The output dimension is c , corresponding to the number of clusters. For $c = 1$, the network outputs a scalar approximating $\sigma_{\mathcal{Y}}(\mathbf{x})$. For $c > 1$, each output $f_{\theta}(\mathbf{x})_j$ approximates $\sigma_{\mathcal{Y}_j}(\mathbf{x})$. At inference, we compute the predicted optimal match for cluster j as $\mathbf{y}_{\text{pred},j} = \nabla_{\mathbf{x}}f_{\theta}(\mathbf{x})_j$ via automatic differentiation. Collectively, the c predicted keys form the rows of the Jacobian matrix $\mathbf{J}_{\mathbf{x}}f_{\theta}(\mathbf{x}) \in \mathbb{R}^{c \times d}$, where the j -th row corresponds to $\nabla_{\mathbf{x}}f_{\theta}(\mathbf{x})_j$. For $c = 1$, this simplifies to $\mathbf{y}_{\text{pred}} = \nabla_{\mathbf{x}}f_{\theta}(\mathbf{x})$.

KeyNet: Direct Key Regression. While SUPPORTNET elegantly leverages convexity, computing gradients at inference adds computational overhead. We propose KEYNET, an architecture that directly outputs an

approximation of the optimal key without requiring gradient computation:

$$\begin{aligned} \mathbf{z}_1 &= \sigma(\mathbf{W}_0^{(x)} \mathbf{x} + \mathbf{b}_0) \in \mathbb{R}^h, \\ \mathbf{z}_{i+1} &= \sigma(\mathbf{W}_i^{(z)} \mathbf{z}_i + \mathbf{W}_i^{(x)} \mathbf{x} + \mathbf{b}_i) \in \mathbb{R}^h, \\ F_\theta(\mathbf{x}) &= \mathbf{W}_L \mathbf{z}_L + \mathbf{b}_L \in \mathbb{R}^{c \times d}. \end{aligned}$$

Unlike SUPPORTNET, we enforce no constraint on the parameters of KEYNET. The output is a $c \times d$ matrix (reshaped from the final layer), where each row $F_\theta(\mathbf{x})_j \in \mathbb{R}^d$ is the predicted optimal key for cluster j . For $c = 1$, the output is simply a d -dimensional vector $F_\theta(\mathbf{x}) \approx \mathbf{y}^*(\mathbf{x})$. While MLP architectures that are guaranteed to output gradients of convex functions have been proposed (Richter-Powell et al., 2021), their implementation is far too complex at the scales (going as far as hundreds of millions of parameters) we consider in this work. Similarly, we have explored using convex regularizers such as the Monge gap (Uscidda and Cuturi, 2023) but given our unusual setting in which ground-truth pairings are known, this did not yield improvements. We explored two additional modifications to these base architectures.

Residual blocks. When enabled, we use ResNet-style residual connections for hidden layers:

$$\mathbf{z}_{i+1} = \mathbf{z}_i + \sigma(\mathbf{W}_i^{(z)} \mathbf{z}_i + \mathbf{W}_i^{(x)} \mathbf{x} + \mathbf{b}_i),$$

when the hidden dimensions of two consecutive states match—this is always the case by default in our setting given the constant hidden dimension. For SUPPORTNET, this modification is convexity-preserving since adding a convex function to the identity (a linear, hence convex, function) yields a convex function. We observe that models using residual blocks take longer to train but can achieve slightly better performance.

Sparse input injection. Rather than injecting the input \mathbf{x} at every layer via $\mathbf{W}_i^{(x)} \mathbf{x}$, we can inject it only at a subset of layers. Let $n_x \in \{0, \dots, L-1\}$ denote the number of layers (after the first) where \mathbf{x} is reinjected. Setting $n_x = 0$ (no injection after the first layer) recovers a standard feedforward architecture.

Network Sizing. We use rectangular (constant-width) networks with hidden dimension h across all L hidden layers. We denote the output dimension $d_{\text{out}} = c$ for SUPPORTNET, $c \cdot d$ for KEYNET, and recall that n_x is the number of times the input is reinjected in the hidden state. The total parameter count amounts to:

- Input projections: $(1 + n_x) \cdot d \cdot h$ (1st layer + n_x)
- Hidden-to-hidden: $(L - 1) \cdot h^2$
- Output layer: $h \cdot d_{\text{out}}$
- Biases: $L \cdot h + d_{\text{out}}$

Given a total **parameter budget** $P := \rho \cdot n \cdot d$, parameterized as a fraction $\rho \leq 1$ of the database size, the dominant constraint is:

$$(L - 1) \cdot h^2 + (1 + n_x)d \cdot h \approx \rho \cdot n \cdot d. \quad (3.2)$$

Solving this quadratic yields, writing $D = (1 + n_x)d$:

$$h \approx \frac{\sqrt{D^2 + 4(L - 1) \cdot P} - D}{2(L - 1)}. \quad (3.3)$$

This formula admits two intuitive limiting cases. For *deep networks* (L large), the h^2 term dominates and $h \approx \sqrt{P/(L - 1)} = \sqrt{\rho \cdot n \cdot d/(L - 1)}$ —width scales as the square root of budget-per-layer. For *shallow networks with frequent reinjection* (n_x large), the linear term dominates and $h \approx P/D = \rho \cdot n/(1 + n_x)$ —width scales linearly with budget, divided among reinjection layers.

Enforcing Homogeneity for SUPPORTNET. The ground-truth support function $\sigma_{\mathcal{Y}}(\mathbf{x})$ is positively 1-homogeneous. To enforce this structure in our SUPPORTNET learned models, we have explored two directions: (1) setting all bias vectors \mathbf{b}_i to zero and using a ReLU activation for σ , which guarantees by construction that property, or (2) relying on a more flexible *homogenization wrapper*: Given any base model $g : \mathbb{R}^d \rightarrow \mathbb{R}$, we define:

$$\mathcal{H}[g](\mathbf{x}) := \|\mathbf{x}\| \cdot g\left(\frac{\mathbf{x}}{\|\mathbf{x}\|}\right). \quad (3.4)$$

This construction guarantees positive 1-homogeneity regardless of the form of g . In practice, we have found this wrapper approach to be more flexible and efficient.

3.2 Loss Functions

A crucial feature of amortized MIPS is that we assume access to a *known* relevant distribution of queries $p_{\mathcal{X}}$, from which we can sample at train time. That distribution *guides* the design of loss functions that optimize model performance for queries drawn from $p_{\mathcal{X}}$, rather than for arbitrary queries. As a result, all expectations below are taken with respect to $\mathbf{x} \sim p_{\mathcal{X}}$, and the model is explicitly tailored to achieve a good performance on that distribution of queries.

Losses for SupportNet. We combine two complementary losses. Let $\mathbf{y}_j^*(\mathbf{x}) = \arg \max_{\mathbf{y} \in \mathcal{Y}_j} \langle \mathbf{x}, \mathbf{y} \rangle$ denote the optimal key for cluster j given query \mathbf{x} . We first consider a *score* regression loss that ensures that the network output approximates the support function for each cluster:

$$\mathcal{L}_{\text{score}}(\theta) = \mathbb{E}_{\mathbf{x} \sim p_{\mathcal{X}}} \left[\frac{1}{c} \sum_{j=1}^c (f_{\theta}(\mathbf{x})_j - \sigma_{\mathcal{Y}_j}(\mathbf{x}))^2 \right].$$

We add to that loss a *gradient matching* term that encourages the gradient to match the optimal key for each cluster:

$$\mathcal{L}_{\text{grad}}(\theta) = \mathbb{E}_{\mathbf{x} \sim p_{\mathcal{X}}} \left[\frac{1}{c} \sum_{j=1}^c \|\nabla_{\mathbf{x}} f_{\theta}(\mathbf{x})_j - \mathbf{y}_j^*(\mathbf{x})\|_2^2 \right].$$

Notice that the minimization of the latter term requires computing (using autodiff) the *cross*-derivatives of $f_{\theta}(\mathbf{x})$ w.r.t \mathbf{x} and then θ . The combined SUPPORTNET objective is a weighted sum of the two.

Losses for KeyNet. We focus first on regressing directly the optimal key, and add a consistency constraint: we first encourage that predicted vectors match their targets:

$$\mathcal{L}_{\text{key}}(\theta) = \mathbb{E}_{\mathbf{x} \sim p_{\mathcal{X}}} \left[\frac{1}{c} \sum_{j=1}^c \|F_{\theta}(\mathbf{x})_j - \mathbf{y}_j^*(\mathbf{x})\|_2^2 \right].$$

and complement that fitting error with a *score consistency* term: Since KEYNET does not output a score directly, but a vector (or a set of vectors), we derive the predicted score as $\langle F_{\theta}(\mathbf{x})_j, \mathbf{x} \rangle$ and penalize deviation from the target score:

$$\mathcal{L}_{\text{consist}}(\theta) = \mathbb{E}_{\mathbf{x} \sim p_{\mathcal{X}}} \left[\frac{1}{c} \sum_{j=1}^c (\langle F_{\theta}(\mathbf{x})_j, \mathbf{x} \rangle - \sigma_{\mathcal{Y}_j}(\mathbf{x}))^2 \right].$$

This consistency loss is motivated by Euler’s theorem for homogeneous functions: if f is positively 1-homogeneous, then $\langle \nabla f(\mathbf{x}), \mathbf{x} \rangle = f(\mathbf{x})$. While KEYNET does not explicitly parameterize a grad-potential, this loss encourages the output to behave as if it were the gradient of a 1-homogeneous function.

3.3 Training Procedure

Before training, we precompute MIPS solutions for queries sampled from $p_{\mathcal{X}}$. For the clustered variant with c clusters, we precompute:

$$\mathcal{D} = \{(\mathbf{x}_i, \{\mathbf{y}_{i,j}^*\}_{j=1}^c)\}_{i=1}^N.$$

from which we can trivially recompute the corresponding scores within each cluster. Here $\mathbf{y}_{i,j}^* = \arg \max_{\mathbf{y} \in \mathcal{Y}_j} \langle \mathbf{x}_i, \mathbf{y} \rangle$ is the optimal key within cluster j for query \mathbf{x}_i . For $c = 1$, this reduces to storing a single optimal key per query. We use exhaustive search for this step.

Query augmentation. Since we have full access to the ground truth generation process, we can easily avoid any limitations on training data through random augmentations of the queries. We have seen that

this improves generalization, and we typically augment training queries with Gaussian noise: $\tilde{\mathbf{x}} = \mathbf{x} + \varepsilon$, $\varepsilon \sim \mathcal{N}(0, \sigma^2 \mathbf{I})$. Note that this requires recomputing all targets for each augmented query.

Activation function. We use a soft leaky ReLU activation:

$$\sigma_{\alpha, \beta}(x) = \alpha x + \frac{(1-\alpha)}{\beta} \log(1 + e^{\beta x}),$$

where α is the negative slope and β controls smoothness. As $\beta \rightarrow \infty$, this approaches the standard leaky ReLU. The fact that the ground-truth support function $\sigma_{\mathcal{Y}}$ is piecewise affine motivates using $\beta \approx \infty$ for SUPPORTNET, but we observe that using $\beta = 20$ strikes a good trade-off between smoothness (better gradient propagation) and adherence to the paradigm. We use $\alpha = 0.1$. While KEYNET should in principle be modeled as a piecewise constant function, we also use the same activation function.

4 Experiments

We evaluate our amortized MIPS approach on retrieval benchmarks, comparing SUPPORTNET (score-based with gradient computation) and KEYNET (direct key regression).

4.1 Experimental Setup

Datasets. We evaluate on four datasets from the BEIR benchmark [Thakur et al. \(2021\)](#): FIQA, Quora, Natural Questions (NQ), and HotpotQA. These corpora ensure robustness across complementary domains and retrieval styles, ranging from financial QA (FIQA) semantic duplicate detection (Quora) to factoid extraction from Wikipedia (NQ) and multi-hop reasoning (HotpotQA). Furthermore, they allow us to assess scalability across order-of-magnitude differences in database size, containing approximately **52K**, **513K**, **2.6M**, and **5.2M** keys, respectively. In all cases, we treat questions as queries and the associated passages or answers as the database keys \mathcal{Y} . All text is encoded into $d = 384$ dimensional L2-normalized embeddings using the general-purpose `all-MiniLM-L6-v2` [Reimers and Gurevych \(2019\)](#) encoder. We use the encoder in an instruction-free manner, passing raw queries and passages without task-specific conditioning. Note that queries and keys differ intrinsically, as queries are short sentences while keys correspond to longer text passages. In other words, in each of these tasks the distribution $p_{\mathcal{X}}$ of queries (embeddings of short questions) differs from that of keys \mathcal{Y} (embedding of long texts).

Data Preparation. Our pre-processing pipeline consists of de-duplication, encoding, and target computation. First, we perform exact string deduplication on both query and document sets. We then encode the unique queries and keys, and augment the resulting *query embeddings* (not the keys) by injecting additive Gaussian noise ($\sigma = 0.02$ based on a preliminary study), expanding the query set by a factor of 5–100× depending on the size of the dataset. The augmented embeddings are re-normalized onto the unit sphere, before being split into train and a small validation set of 1000 vectors used to produce all evaluation metrics shown hereafter. Finally, for every query, we compute the top- k retrieved candidates from the database via exact MIPS. The indices of the maximal inner-product solutions serve as the ground-truth targets for supervision during training. For clustering-based experiments, we further partition the database using k -means and compute the optimal keys within each cluster.

Architecture Configuration & Training. Both SUPPORTNET and KEYNET use rectangular (constant-width) networks inferred from rule [equation 3.3](#) using:

- **Depth:** $L \in \{4, 8, 16\}$ hidden layers
- **Parameters fraction:** $\rho \in \{\mathbf{XS} = 1\%, \mathbf{S} = 5\%, \mathbf{M} = 10\%, \mathbf{L} = 20\%, \mathbf{XL} = 40\%, \mathbf{XXL} = 50\%\}$ of $n \times d$ database size.
- **Passthrough:** n_x , total input skip connections

We always apply the Homogenize wrapper to SUPPORTNET to enforce positive 1-homogeneity. We train models with Adam using a cosine learning rate schedule with warmup (2.5% of training horizon) and peak value at $\approx 10^{-4}$. For both models, we emphasize the key reconstruction as training signal: we use $\lambda_{\text{score}} = 0.01$

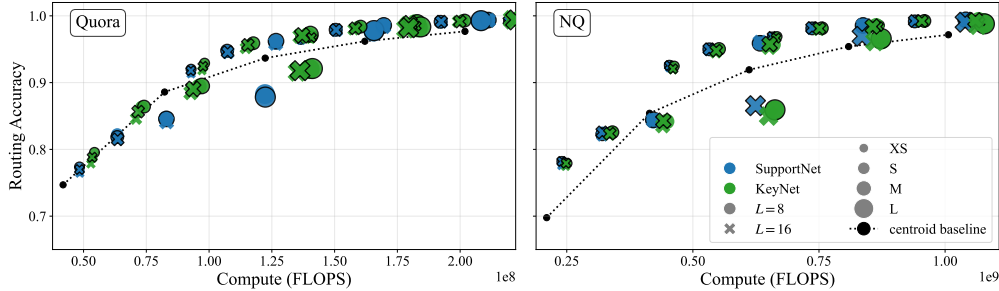


Figure 2 Results for the routing experiment described in Section 4.4, on **Quora** (left, $n \approx 500k$) and **NQ** (right, $n \approx 2.5M$). Here SUPPORTNET and KEYNET are used to predict the support function of a query on $c = 10$ clusters of the entire set of keys \mathcal{Y} , followed by exhaustive search within the top scored cluster. For the baseline clustering approach, the cluster is selected first using the top-scoring centroid to the query. These results show that multiple models (trained with various variants of depth L , size ρ , peak learning rate etc.) achieve consistently a better routing accuracy with a lower FLOPS budget, highlighting the stability of the performance of SUPPORTNET and KEYNET training pipelines to various hyperparameters. Our recommendation, in any practical deployment scenario, would be to select one of those very best performing models depending on the trade-off sought in practice. Markers outlined with a black line correspond to settings in which the input \mathbf{x} is re-injected every 4 layers ($n_x \approx L/4$) whereas no outline indicates reinjection at every layer ($n_x = L$).

and $\lambda_{\text{grad}} = 1.0$ for SUPPORTNET; $\lambda_{\text{key}} = 1.0$ and $\lambda_{\text{consist}} = 0.01$ for KEYNET. We track the EMA of model parameters (decay 0.999 for batch size 128) and use EMA parameters for evaluations. The batch sizes we use range from 512 to 16384 depending on the dataset size. We find that a size of 4096 reaches a good trade-off of performance vs. throughput when training. We rescale the learning rate using the square-root ratio to reference batch size, and scale the EMA decay geometrically with batch-size (Busbridge et al., 2023). See Table 1 in appendix for the time needed (per sample) to recover both support and key from a query for these networks.

4.2 Metrics

Apart from regression losses (to score/key, respectively) and matching terms (gradient/consistency), we evaluate both SUPPORTNET and KEYNET models using two metrics:

Relative Transport Error. Since our goal is to learn a transport map $\mathbf{x} \mapsto \mathbf{y}^*(\mathbf{x})$, we introduce a *relative* error metric that measures prediction quality relative to the baseline distance between query and target. We write here $\hat{\mathbf{y}}(\mathbf{x})$ for the predicted key of our models, either $\nabla_{\mathbf{x}} f_{\theta}(\mathbf{x})$ for SUPPORTNET and $F_{\theta}(\mathbf{x})$ for KEYNET, and define

$$\mathcal{E}_{\text{rel}} = \left(\mathbb{E}_{\mathbf{x}} \left[\log \frac{\|\hat{\mathbf{y}}(\mathbf{x}) - \mathbf{y}^*\|_2^2}{\|\mathbf{x} - \mathbf{y}^*\|_2^2} \right] \right), \quad (4.1)$$

When the number of clusters $c > 1$, that metric is computed per key-in-cluster prediction, and averaged. This log-ratio measures how much closer (negative values) or farther (positive values) the prediction is to the target compared to the query itself. A value of $\mathcal{E}_{\text{rel}} = 0$ means the prediction error equals the query-to-target squared-distance; $\mathcal{E}_{\text{rel}} = -1$ means the prediction is $e^{-1} \approx 0.37\times$ as far from the target as the query is. In other words, the relative transport error (RTE) $\exp(\mathcal{E}_{\text{rel}})$ is the geometric average of the ratio of the squared norms between prediction to ground-truth key and query to ground-truth key. We observe that our models start performing well when \mathcal{E}_{rel} goes below -1 . The training dynamics for that metric are shown in Figure 8.

Retrieval Metrics. We track whether the location of the predicted key $\hat{\mathbf{y}}(\mathbf{x})$ agrees, relative to all other keys, with the original query. The *match rate* is the fraction of queries where $\arg \min_{\mathbf{y} \in \mathcal{Y}} \|\hat{\mathbf{y}} - \mathbf{y}\| = \mathbf{y}^*$. *Recall@k* is the fraction of queries where \mathbf{y}^* is among the k nearest neighbors of $\hat{\mathbf{y}}$. The *mean reciprocal rank* (MRR) is the mean reciprocal rank of \mathbf{y}^* in the ranking induced by distance from $\hat{\mathbf{y}}$.

Notice that the relative transport error and retrieval metrics can agree jointly when the prediction is perfect, but do not necessarily agree in other cases. For instance, if the predictor $\hat{\mathbf{y}}$ were simply initialized to be

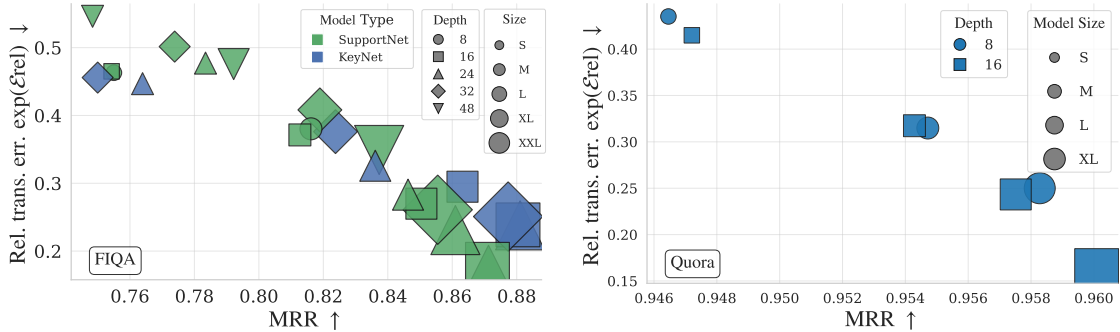


Figure 3 \mathcal{E}_{rel} vs. MRR metric on various model sizes and depths for SUPPORTNET and KEYNET at the end of training on FIQA (*left*) and QUORA (*right*, only KEYNET reported on that task as used later in Section 4.5). Lower right corner (i.e., high MRR and low \mathcal{E}_{rel}) is best.

the identity, the RTE would be equal to 1, whereas matching metrics would give the best possible values, by definition. During our training, we have therefore tracked models that are able to transport significantly close to target (RTE ≈ 0) while maintaining good metrics.

4.3 Training Trade-offs: MRR vs. \mathcal{E}_{rel}

The tradeoffs achieved on both relative transport error vs. retrieval metrics achieved by our trained models are shown in Figure 3 for two datasets, FIQA (50k) and QUORA (500k). As can be seen, the size (ranging from XS to XXL) directly impacts the quality of the prediction of the model.

4.4 Performance as Routing Mechanism

We evaluate the clustered variant ($c > 1$) where the model simultaneously learns support functions for multiple database partitions. This enables a two-stage search strategy: use the learned scores to identify the top- k most promising clusters, then perform exact search within those clusters.

Setup. We begin by clustering the Quora and NQ datasets into $c = 10$ clusters centered around centroids $\{\mathbf{z}_i\}_{i=1}^c$ using k-means. We run clustering end-to-end 10 times and select the clustering which yields the most even cluster sizes, in order to balance the cost of exact search within each cluster. We then train SUPPORTNET and KEYNET models using $c = 10$, following the conventions in Section 4.1. To obtain a Pareto frontier, we vary the number of clusters k searched at test time, going from only the top-1 cluster up to top-5. For the baseline, we perform routing by comparing the query \mathbf{q} against the cluster centroids \mathbf{z}_i ; that is, we predict $\arg \max_i \langle \mathbf{q}, \mathbf{z}_i \rangle$. We then evaluate each method in terms of *routing accuracy* (whether the target key is in the selected clusters) versus *compute* (total number of flops needed to perform cluster selection and exact search within the selected clusters).

Results. On NQ, both SUPPORTNET and KEYNET consistently beat out the baseline at all budgets, yielding a ≥ 10 point increase at $k = 1$ with minimal overhead and saturating close to 100% routing accuracy at $k = 5$. These performance gains are evident for models of larger size (M, L), which dominate on this dataset. Meanwhile, on the smaller Quora set of queries—thus exact search within each cluster is cheaper—the baseline performs favorably in the low cost regime, but SUPPORTNET and KEYNET scale better with increased compute. Here, smaller model sizes (XS, S) instead dominate. As to the choice of SUPPORTNET vs. KEYNET, we observe that both models perform similarly at most sizes, with slight performance gains across the board for KEYNET. However, on Quora the increased size of the final output layer of KEYNET ($h \times cd$) compared to that of SUPPORTNET ($h \times c$) affects the total flop count more strongly. SUPPORTNET thus becomes competitive when compute is limited. Generally speaking, we observe that dense re-injections (i.e. n_x close to L) and increasing depth L do not affect the performance significantly, but may nonetheless impact training stability.

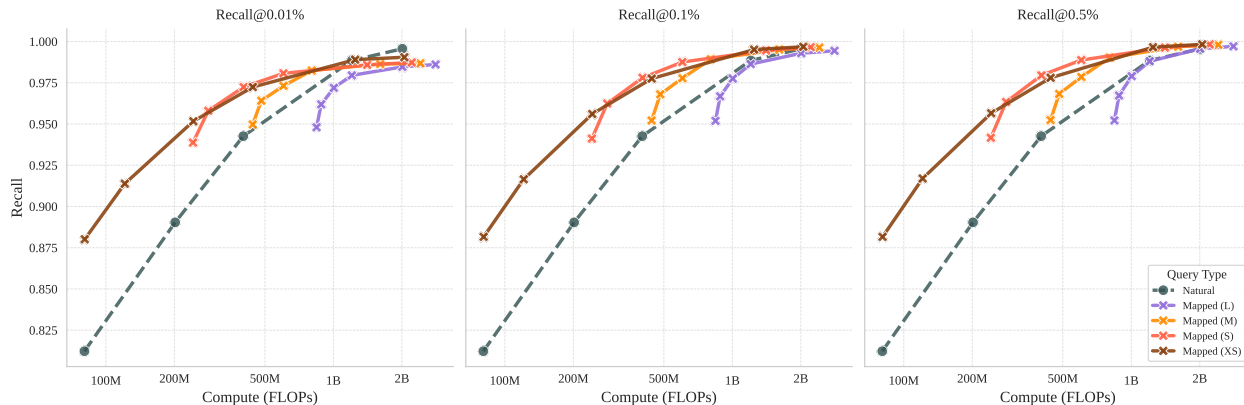


Figure 4 Results for approximate search integration as described in Section 4.5. We use KEYNET to predict the actual top key for \mathbf{x} found in the entire **HotpotQA** set of $\approx 5.2\text{M}$ keys, and run approximate search with a FAISS IVF index. We then query the database with $\hat{\mathbf{y}}(\mathbf{x})$ instead of \mathbf{x} under growing search budgets. Compared to submitting directly the prompt to FAISS, our approaches always pay a forward cost price needed to evaluate the prediction (which grows roughly linearly with ρ , model size) and then run fast MIPS search on that prediction with varying number of n_{probe} , collecting cumulated FLOPs count for our method, and raw flop counts for FAISS when applied directly on \mathbf{x} . Note that 0.01% is here equivalent to a recall at approximately 500 given the original size of **HotpotQA**.

4.5 Approximate Search Integration

In this section, we focus on compressing a single dataset of keys, i.e. $c = 1$, and focus on top key retrieval. Because SUPPORTNET requires a backward pass to output that prediction, its FLOPs overhead (starting from the same total parameter count) compared to KEYNET is prohibitive (the backward pass costs typically 1-2 times more than the forward). As a result, we focus on KEYNET in this section. We integrate KEYNET into an Inverted File (IVF) index structure Johnson et al. (2019), a standard method for approximate nearest neighbor search. The IVF index partitions the database \mathcal{Y} into Voronoi cells (clusters) based on a coarse quantization of the embedding space. Retrieval operates in two stages: identifying the n_{probe} clusters closest to the query vector, and performing an exact search only within those specific partitions. We compare two retrieval strategies: **Natural**: Querying the index using the original query vector \mathbf{x} vs. **Mapped**: Querying the index using the predicted key vector $\hat{\mathbf{y}}$. We assess the trade-off between retrieval accuracy and computational cost by sweeping the search budget. Specifically, we increment the number of probes (n_{probe}), effectively increasing the fraction of the database exhaustively searched. By plotting Recall@ k against the search budget, we measure whether mapping queries toward their ground-truth keys allows the index to locate the correct partition more efficiently, thereby achieving higher recall with fewer floating-point operations.

5 Conclusion

We have introduced *amortized MIPS*, a learning-based paradigm to train neural networks to directly predict MIPS solutions on a distribution of queries that matter to the end-user. Our approach exploits the mathematical structure of MIPS: the value function is the *support function* of the database—a convex, positively 1-homogeneous function whose gradient equals the optimal key. We explored two complementary architectures. SUPPORTNET learns the convex support function using relaxed ICNNs and recovers matches via (automatically differentiated) gradients, naturally aligning with the problem’s mathematical structure. KEYNET directly regresses the optimal key, bypassing gradients entirely at inference and resulting in a simpler training dynamic. Both architectures extend naturally to the clustered setting, where we simultaneously learn support functions for multiple database partitions.

Limitations and future work. Our approach requires a representative query distribution \mathcal{X} for training; performance may degrade for out-of-distribution queries. Scaling to very large databases (billions of vectors) will require scaling up our pre-computation procedure to incorporate more efficient pre-processing and dataloaders. Future work could explore online learning to adapt to query distribution shift or distillation from

larger models.

The amortized perspective of AMIPS opens new directions for learned retrieval. By encoding MIPS solutions in neural network weights, we trade one-time training cost for fast inference, making this approach attractive for latency-sensitive applications with predictable query patterns.

References

- Yoram Bachrach, Yehuda Finkelstein, Ran Gilad-Bachrach, Liran Katzir, Noam Koenigstein, Nir Nice, and Ulrich Paquet. Speeding up the xbox recommender system using a euclidean transformation for inner-product spaces. In *ACM Conference on Recommender Systems*, 2014. URL <https://api.semanticscholar.org/CorpusID:11381549>.
- Noam Koenigstein, Parikshit Ram, and Yuval Shavitt. Efficient retrieval of recommendations in a matrix factorization framework. In *Proceedings of the 21st ACM International Conference on Information and Knowledge Management*, pages 535–544, 2012.
- Anshumali Shrivastava and Ping Li. Asymmetric lsh (alsh) for sublinear time maximum inner product search (mips). In *Advances in Neural Information Processing Systems*, 2014.
- Ruiqi Guo, Sanjiv Kumar, Krzysztof Choromanski, and David Simcha. Quantization based fast inner product search. In *Proceedings of the 19th International Conference on Artificial Intelligence and Statistics*, 2016.
- Wenlin Chen, James Wilson, Stephen Tyree, Kilian Weinberger, and Yixin Chen. Compressing neural networks with the hashing trick. In *International Conference on Machine Learning*, pages 2285–2294, 2015.
- Hervé Jégou, Matthijs Douze, and Cordelia Schmid. Product quantization for nearest neighbor search. *IEEE Transactions on Pattern Analysis and Machine Intelligence*, 2011.
- Brandon Amos, Lei Xu, and J Zico Kolter. Input convex neural networks. *Proceedings of the 34th International Conference on Machine Learning*, 2017.
- Behnam Neyshabur and Nathan Srebro. On symmetric and asymmetric lshs for inner product search. In *International Conference on Machine Learning*, 2015.
- Ruiqi Guo, Philip Sun, Erik Lindgren, Quan Geng, David Simcha, Felix Chern, and Sanjiv Kumar. Accelerating large-scale inference with anisotropic vector quantization. *Proceedings of the 37th International Conference on Machine Learning*, pages 3887–3896, 2020.
- Stanislav Morozov and Artem Babenko. Non-metric similarity graphs for maximum inner product search. In *Advances in Neural Information Processing Systems*, 2018.
- Yu A. Malkov and Dmitry A. Yashunin. Efficient and robust approximate nearest neighbor search using hierarchical navigable small world graphs. *IEEE Transactions on Pattern Analysis and Machine Intelligence*, 2020. doi: 10.1109/TPAMI.2018.2889473.
- Xinyan Dai, Xiao Yan, Kelvin KW Ng, Jiu Liu, and James Cheng. Norm-explicit quantization: Improving vector quantization for maximum inner product search. In *Proceedings of the AAAI Conference on Artificial Intelligence*, 2020.
- Fumin Shen, Wei Liu, Shaoting Zhang, Yang Yang, and Heng Tao Shen. Learning binary codes for maximum inner product search. In *International Conference on Computer Vision (ICCV)*, 2015. doi: 10.1109/ICCV.2015.472.
- Tim Kraska, Alex Beutel, Ed H. Chi, Jeffrey Dean, and Neoklis Polyzotis. The case for learned index structures. In *Proceedings of the 2018 International Conference on Management of Data, SIGMOD*, 2018. doi: 10.1145/3183713.3196909.
- Yize Chen, Yuanyuan Shi, and Baosen Zhang. Optimal control via neural networks: A convex approach. In *International Conference on Learning Representations, ICLR*, 2019.
- Pieter-Jan Hoedt and Günter Klambauer. Principled weight initialisation for input-convex neural networks. *Advances in Neural Information Processing Systems*, 36:46093–46104, 2023.
- Yann Brenier. Polar factorization and monotone rearrangement of vector-valued functions. *Communications on Pure and Applied Mathematics*, 44(4):375–417, 1991.

- Ashok Vardhan Makkuva, Amirhossein Taghvaei, Sewoong Oh, and Jason D. Lee. Optimal transport mapping via input convex neural networks. 2020.
- Alexander Korotin, Lingxiao Li, Aude Genevay, Justin Solomon, Alexander Filippov, and Evgeny Burnaev. Do Neural Optimal Transport Solvers Work? A Continuous Wasserstein-2 Benchmark. In *NeurIPS*, 2021.
- Brandon Amos. Amortizing convex conjugates for optimal transport. In *International Conference on Learning Representations*, 2023.
- Charlotte Bunne, Andreas Krause, and Marco Cuturi. Supervised training of conditional Monge maps. In *Advances in Neural Information Processing Systems*, volume 35, pages 6859–6872, 2022.
- Alexander Korotin, Daniil Selikhanovych, and Evgeny Burnaev. Neural optimal transport. In *International Conference on Learning Representations, ICLR*, 2023.
- R Tyrrell Rockafellar. *Convex analysis*. Number 28. Princeton university press, 1970.
- Jean-Baptiste Hiriart-Urruty and Claude Lemaréchal. *Fundamentals of Convex Analysis*. Springer Science & Business Media, 2004.
- Jack Richter-Powell, Jonathan Lorraine, and Brandon Amos. Input convex gradient networks. *arXiv preprint arXiv:2111.12187*, 2021.
- Théo Uscidda and Marco Cuturi. The monge gap: A regularizer to learn all transport maps. In Andreas Krause, Emma Brunskill, Kyunghyun Cho, Barbara Engelhardt, Sivan Sabato, and Jonathan Scarlett, editors, *Proceedings of the 40th International Conference on Machine Learning*, volume 202 of *Proceedings of Machine Learning Research*, pages 34709–34733. PMLR, 23–29 Jul 2023. URL <https://proceedings.mlr.press/v202/uscidda23a.html>.
- Nandan Thakur, Nils Reimers, Andreas Rücklé, Abhishek Srivastava, and Iryna Gurevych. BEIR: A heterogeneous benchmark for zero-shot evaluation of information retrieval models. In *Thirty-fifth Conference on Neural Information Processing Systems Datasets and Benchmarks Track*, 2021.
- Nils Reimers and Iryna Gurevych. Sentence-bert: Sentence embeddings using siamese bert-networks. In *Proceedings of the 2019 Conference on Empirical Methods in Natural Language Processing*. Association for Computational Linguistics, 11 2019. URL <https://arxiv.org/abs/1908.10084>.
- Dan Busbridge, Jason Ramapuram, Pierre Ablin, Tatiana Likhomanenko, Eeshan Gunesh Dhekane, Xavier Suau Cuadros, and Russell Webb. How to scale your ema. *Advances in Neural Information Processing Systems*, 36: 73122–73174, 2023.
- Jeff Johnson, Matthijs Douze, and Hervé Jégou. Billion-scale similarity search with GPUs. *IEEE Transactions on Big Data*, 7(3):535–547, 2019.

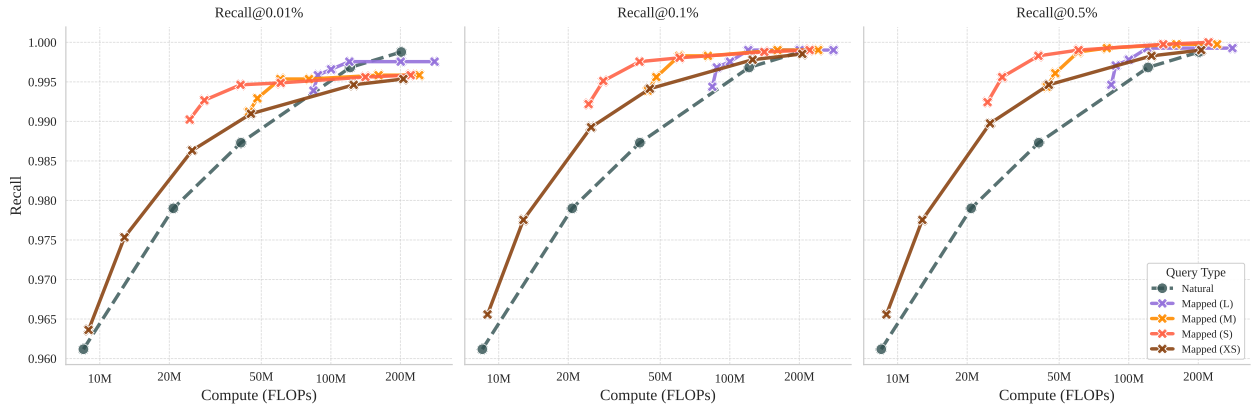


Figure 5 Results for approximate search integration as described in Section 4.5 on Quora.

A Appendix

A.1 Timing Results

In Table 1 we compare the time to compute scores and gradient using SUPPORTNET and KEYNET across dataset sizes and model parameter fractions. For gradient computation, SUPPORTNET requires backpropagation through the network, while KEYNET directly predicts the gradients, resulting in gradient times that closely match the score times.

Dataset	Parameter Fraction	SUPPORTNET		KEYNET	
		Score	Grad	Score	Grad
Quora (513K)	0.05 (S)	1.34×10^{-3}	2.50×10^{-3}	1.28×10^{-3}	1.29×10^{-3}
	0.1 (M)	2.18×10^{-3}	4.08×10^{-3}	2.13×10^{-3}	2.12×10^{-3}
	0.2 (L)	1.99×10^{-3}	3.12×10^{-3}	1.90×10^{-3}	1.90×10^{-3}
Natural Questions (2.6M)	0.05 (S)	4.56×10^{-3}	8.64×10^{-3}	4.46×10^{-3}	4.46×10^{-3}
	0.1 (M)	8.55×10^{-3}	1.62×10^{-2}	7.68×10^{-3}	7.69×10^{-3}
	0.2 (L)	7.08×10^{-3}	1.23×10^{-2}	6.00×10^{-3}	5.99×10^{-3}
HotpotQA (5.2M)	0.05 (S)	8.69×10^{-3}	1.68×10^{-2}	8.15×10^{-3}	8.15×10^{-3}
	0.1 (M)	1.59×10^{-2}	3.05×10^{-2}	1.49×10^{-2}	1.49×10^{-2}
	0.2 (L)	3.14×10^{-2}	5.96×10^{-2}	2.85×10^{-2}	2.86×10^{-2}

Table 1 Timing comparison between SUPPORTNET and KEYNET across datasets and parameter fractions. *Score* and *Grad* columns show the time in seconds required to process a batch of 4096 queries in dimension 384, averaged over 100 runs. Number of keys for each dataset is shown in parentheses.

A.2 FAISS Integration of KeyNet Retrieval Methods

We plot approximate search performance under varying budget for Quora and Natural Questions on Figures 5 and 6, respectively.

A.3 Robustness to out-of-distribution queries

We tested XS variants of KEYNET on perturbed versions of the test of HotPotQA. Perturbations follow the scheme discussed in Section 4.1, used for augmenting training data; we apply Gaussian noise and re-normalize query representations. In this case however, we made it so noise distributions differ relative to those used to prepare training so there are significant distribution shifts on the test query distributions with respect to the source of training queries.

As one would expect, learning-based approaches degrade in performance under distribution shifts, as can be

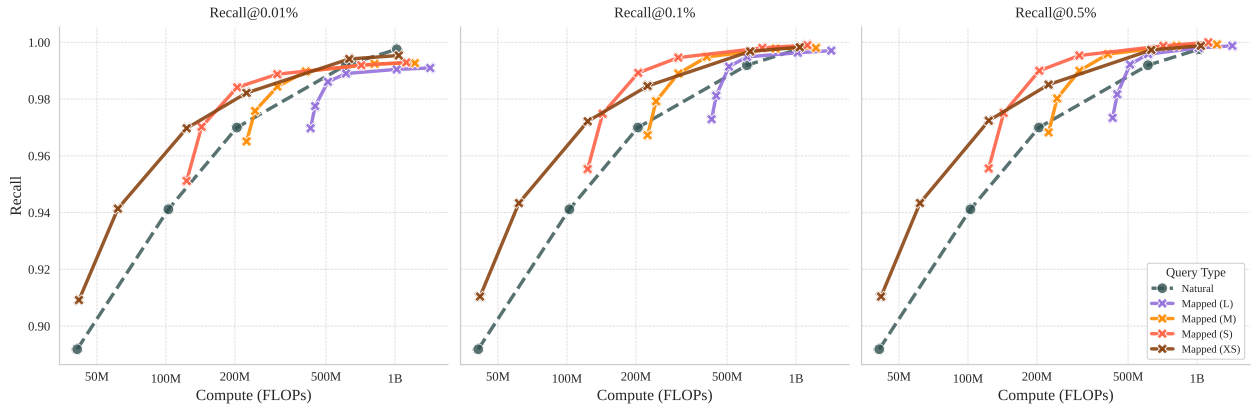


Figure 6 Results for approximate search integration as described in Section 4.5 on Natural Questions NQ.

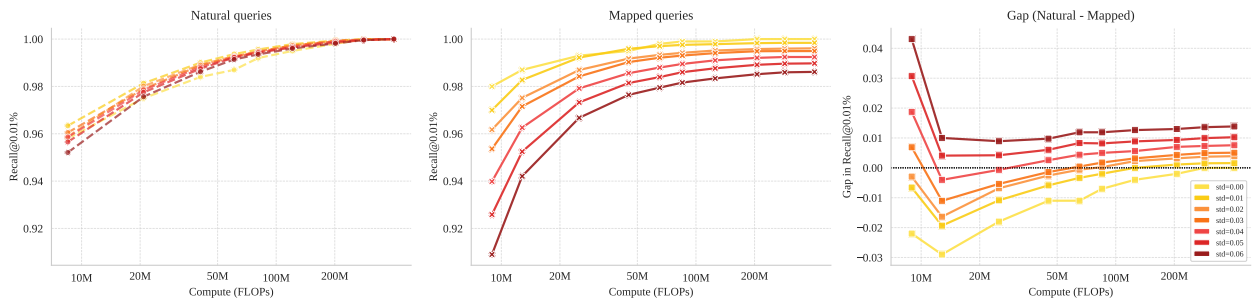


Figure 7 Evolution of the MRR vs. search cost due to increasing distribution shift in the query test distribution on HotPotQA (i.e., under growing Gaussian noise standard deviation, std). Both natural (*left*) and mapped (*center*) queries incur degradation under noisy queries. The gap (natural-mapped) in the *right* plot (lower than 0 means that our approach outperforms the baseline) is more pronounced in the extrema of the search compute budgets we considered.

seen in Figure 7. Interestingly however, degradation is not catastrophic and models still achieve a relatively high recall in absolute terms even under much higher noise levels that what was observed during training; although the gap with respect to natural queries is significant, especially so at very low or very high compute scenarios where the gaps are more pronounced. This can likely be alleviated by more aggressive data augmentation, but wouldn't render models robust to other types of distribution shifts.

A.4 Training Dynamics

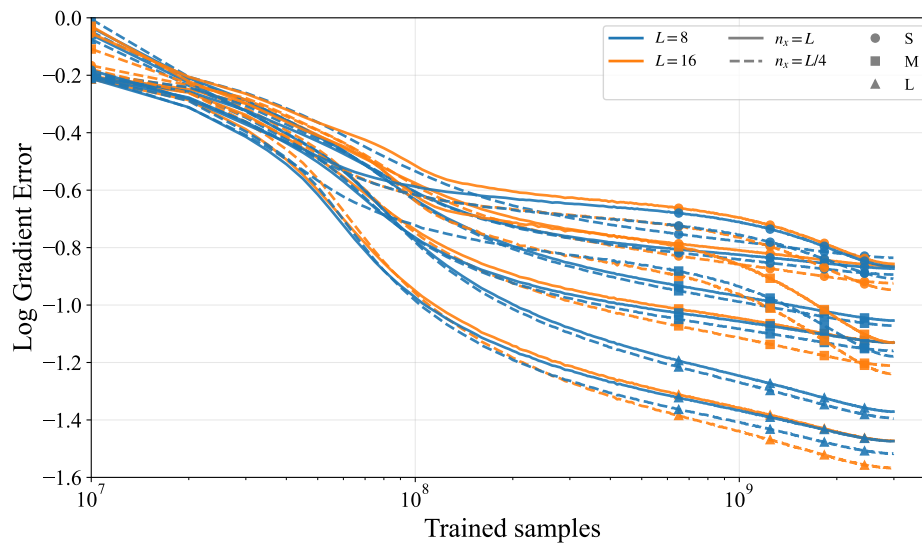


Figure 8 Evolution of the relative transport error \mathcal{E}_{rel} during training on **Quora** for KEYNET across different model sizes. Lower values indicate predictions closer to the ground-truth key. Larger models achieve lower final error and favor greater depth.